

Denison University

Denison Digital Commons

Student Scholarship

2024

Uncovering the Brightening Effect in Mn-Doped Cs₃Bi₂Br₉ Nanoplatelets

Lauren Rutherford
Denison University

Follow this and additional works at: <https://digitalcommons.denison.edu/studentscholarship>

Recommended Citation

Rutherford, Lauren, "Uncovering the Brightening Effect in Mn-Doped Cs₃Bi₂Br₉ Nanoplatelets" (2024).
Student Scholarship. 245.
<https://digitalcommons.denison.edu/studentscholarship/245>

This Thesis is brought to you for free and open access by Denison Digital Commons. It has been accepted for inclusion in Student Scholarship by an authorized administrator of Denison Digital Commons. For more information, please contact eresources@denison.edu.

Uncovering the Brightening Effect in Mn-Doped Cs₃Bi₂Br₉ Nanoplatelets

Lauren Rutherford

Project Advisor: Dr. Tim Atallah

Department of Chemistry and Biochemistry

Copyright

Permission to make digital/hard copy of part or all of this work for personal or classroom use is granted without fee provided that the copies are not made or distributed for profit or commercial advantage, the copyright notice, the title of the work, and its date appear, and notice is given that copying is by permission of the author. To copy otherwise, to republish, to post on a server, or to redistribute to lists, requires prior specific permission of the author and/or a fee. (Opinions expressed by the author do not necessarily reflect the official policy of Denison University.)

Copyright, Lauren Rutherford, 2024

Uncovering the Brightening Effect in Mn-Doped Cs₃Bi₂Br₉ Nanoplatelets

Lauren Rutherford

Department of Chemistry and Biochemistry

Advisor: Dr. Atallah

Abstract

Colloidal nanocrystal semiconductors are of interest due to size and shape tunability allowing control of electronic structure and their low temperature solution synthesis. Cs₃Bi₂Br₉ nanocrystals are particularly appealing due to the lack of toxic heavy metals, straightforward synthesis, and photo/thermal stability. However, Cs₃Bi₂Br₉ nanocrystals show relatively low quantum yields, limiting their optoelectronic applicability. Here we show that introducing Mn²⁺ dopants to Cs₃Bi₂Br₉ colloidal nanocrystals results in a broad, visible emission that increases in intensity while under laser illumination. This brightening effect may be caused by a matrix that forms between the glass substrate and Cs₃Bi₂Br₉:Mn film as it is heated due to high laser power.

Acknowledgments

I would like to thank Dr. Atallah, all of the former and current Atallah lab members, Jody Cambraia, Dr. Quintin Cheek, and the Department of Chemistry and Biochemistry. Additionally, I am extremely appreciative of funding from the Lisska Center's Student Research Fund and the Anderson Summer Science Program.

TABLE OF CONTENTS

Introduction	6
Experimental Rationale	9
Experimental Methods	10
Results	11
Discussion	14
Future Work	16
References	18

INTRODUCTION

General Introduction

Metal halide perovskites (MHPs) were initially discovered in 1893, however, it wasn't until the 1990s that this material began to garner interest for light-emitting devices and transistors.¹ The bulk MHPs were found to have charge transport properties in 2012, however, their photoluminescence quantum yield (PLQY) is limited due to mobile ionic defects being present and small exciton binding energies.¹ These limitations lead to a transition to MHP nanocrystals (NCs) which were first synthesized in 2014 as a way to boost PLQY by using quantum confinement sizes as another method for tuning emission.¹ These MHP NCs used organic capping ligands to allow for growth in the nanometer size range with the ability to tune size and shape to create different nanostructures such as nanoplatelets, nanosheets, nanowires, and quantum dots.¹ There have been rapid advances in the synthesis of perovskite NCs in the past 10 years with Schmidt et al. making MAPbBr₃ NCs with PLQY of 20% in 2013 and Protesescu et al. developing the colloidal synthesis of monodisperse CsPbX₃ NCs in 2015 which led to the adoption of the standard hot injection method.^{2,3}

During this time, two different synthesis methods were developed, hot injection and ligand-assisted reprecipitation (LARP) as the research surrounding perovskite nanocrystals increased. The hot injection method was originally developed to synthesize cadmium chalcogenide nanocrystals and LARP is a process of supersaturated recrystallization which dates back to more than 5000 years ago.¹ The hot injection method involves the injection of the cation precursor solution into a solution of ligands, anion, and halide followed by an ice bath as shown in Figure 1. Its advantages include

generally smaller NCs with less of a variance in size, easy manipulation of size, size distribution, and shape through precursor to ligand ratios, injection temperature, reaction time, and precursor concentration.¹ However, this method isn't scalable as the Cs-oleate (or similar solution) has to be made and preheated separately before injection and the synthesis usually has to be carried out in an inert atmosphere.¹ LARP synthesis is a response to this issue as it can be carried out in the air using facile techniques. It involves the injection of the ligands and metal halide salts dissolved in a “good” solvent into a “bad” solvent to induce the nucleation of NCs as shown in Figure 1. Although, fewer lead-free perovskite nanocrystals have been reported using this method and the polar solvents that would normally be used in a LARP synthesis can degrade the NCs.¹

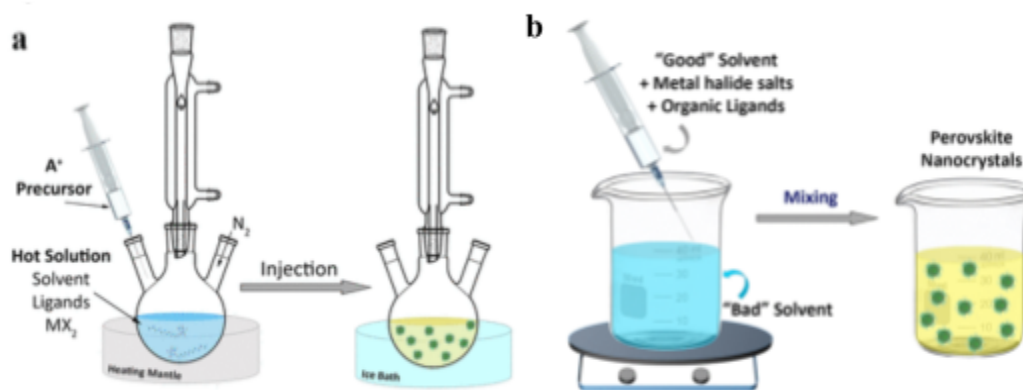


Figure 1: Depiction of hot injection (a) and LARP (b) synthesis methods. Adapted from Ref. 1.

Project Introduction

There has been a lot of effort in recent years looking at lead-free halide perovskite options, for example, Sn^{II} , Sn^{IV} , Sb^{III} , Bi^{III} , Pd^{IV} , Cu^{II} , In^{III} , and Ag^{I} have been employed to replace Pb and yield lead-free halide perovskite nanocrystals.⁴ Lead halide perovskites follow the general formula of APbX_3 (where $\text{A} = \text{CH}_3\text{NH}_3^+$ (MA), $\text{CH}(\text{NH}_2)^{2+}$ (FA) or Cs^+ ; $\text{X} = \text{Cl}$, Br , or I) and when replacing Pb with a neighboring element, such as Bi and

Sb, $A_3B_2X_9$ (where B = Bi or Sb) becomes the more stable stoichiometry with two main polymorphs depending on the synthesis method.⁴ However the solar cell power conversion efficiencies (PCEs) of these Bi and Sb-based MHPs are only around 2-3% compared to the 23% PCE of Pb-based perovskites. On the other hand, the lead-free MHPs show relatively better stability.⁵

Another method to change the properties of the MHP NCs is doping, which broadly means the introduction of specified impurity ions in the host. Specifically in perovskites doping means the partial replacement of one of the original elements with specific ions.⁶ In particular Mn^{2+} has been studied as a dopant for MHP NCs, and semiconductor NCs in general because it has the potential to introduce magnetic and optical properties to the NC.^{6,7}

The goal of my research was to introduce a dopant into a lead-free perovskite or perovskite adjacent material. $Cs_3Bi_2Br_9$ nanoplatelets offer straightforward synthesis and photo/thermal stability, however, they show relatively low quantum yields which limits their optoelectronic potential.⁸

Preliminary Work

Initial research focused on successfully synthesizing $Cs_3Bi_2Br_9$ nanoplatelets via the method developed by Creutz et al. and being able to reproduce the results found in the literature (Fig. 2).⁸ The next step was beginning to incorporate dopants, adding impurities to the

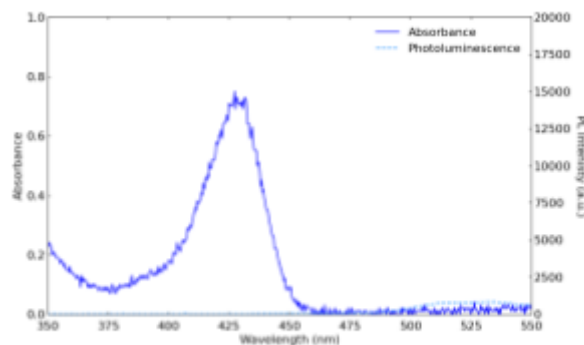


Figure 2: Absorbance and photoluminescence spectra of $Cs_3Bi_2Br_9$ nanoplatelets that is consistent with the literature.

Cs₃Bi₂Br₉ nanoplatelets in an attempt to improve the quantum yields of the material. While completing summer research it was found that manganese-doped (Mn-doped) Cs₃Bi₂Br₉ nanoplatelets had a brighter emission that increased in intensity while under laser illumination, as shown in Figure 3.

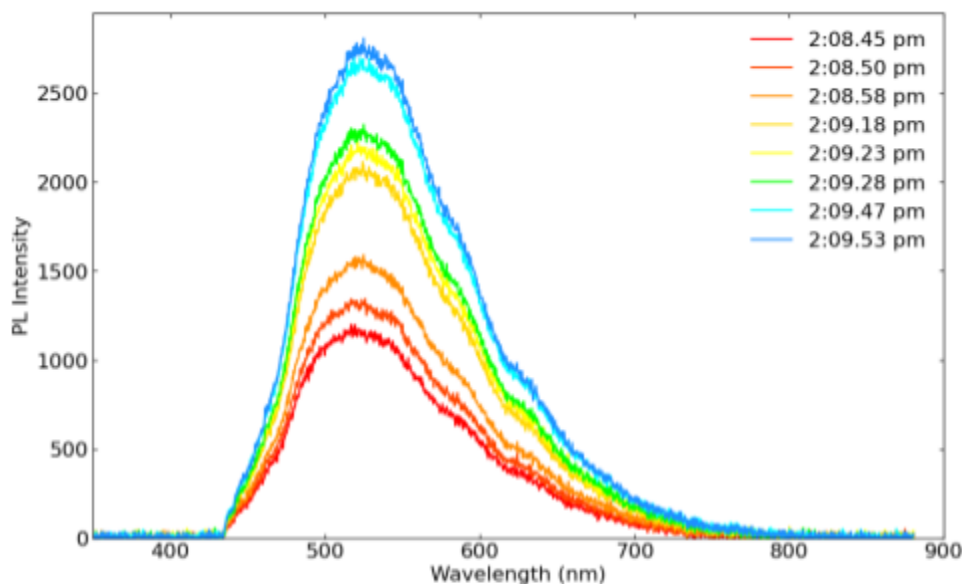


Figure 3: The intensity of photoluminescence (brightness) increasing as time passes while being excited at 405 nm.

EXPERIMENTAL RATIONALE

Two hypotheses were developed to explain the brightening effect, described as thermal annealing and energy shelving. The first hypothesis, thermal annealing, describes an irreversible chemical change that gets rid of defect states present in the material because as the material is given energy, the atoms are able to move to a more ideal arrangement which would increase the material's emission. The second hypothesis, energy shelving, would be the buildup of electrons in Mn²⁺ dopant state because they are being excited faster than they can be emitted. In order to test these hypotheses, kinetics experiments

and analysis of brightening and dimming, a control annealing experiment, a reversibility experiment, and the ability to correlate the thickness of the sample with absorbance and photoluminescence intensity were needed. However, once a dark spot on the film after extended laser illumination was noticed, new experiments were required. Energy dispersive x-ray spectroscopy (EDS) with elemental analysis and images using scanning electron microscopy (SEM) were needed to understand the makeup and characteristics of the dark spot.

EXPERIMENTAL METHODS

Mn-doped $\text{Cs}_3\text{Bi}_2\text{Br}_9$ nanoplatelets were synthesized using a variation of the hot injection method developed by Creutz et al. with the addition of manganese (II) acetate. The method involved injecting bromotrimethylsilane (TMS-Br) into a solution of cesium acetate, bismuth acetate, manganese (II) acetate, octadecene, oleylamine, and oleic acid that was heated to 160°C (Fig. 4). The undoped nanoplatelets were also synthesized for comparison using the same method, excluding the manganese (II) acetate.

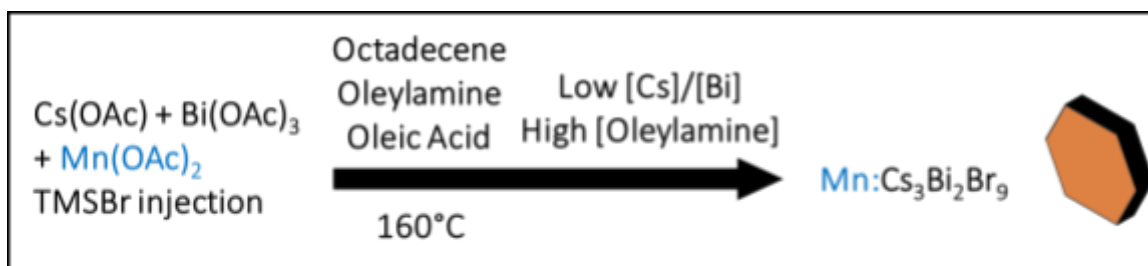


Figure 4: Description of the Mn-doped $\text{Cs}_3\text{Bi}_2\text{Br}_9$ synthesis process that involves the addition of manganese (II) acetate.

After synthesis, the nanoplatelets were isolated through a workup process that used hexane as a solvent, centrifugation that was repeated three times for thirty minutes at 6000 rpm each time, and the sonication of the precipitate for at least 5 minutes before

measurements were taken. Films of the nanoplatelets were then made by drop casting the $\text{Cs}_3\text{Bi}_2\text{Br}_9\text{:Mn}$ hexane solution on coverslips with epoxy borders that were added to increase the thickness of the films.

To characterize the extent of manganese doping in the hexagonal $\text{Cs}_3\text{Bi}_2\text{Br}_9$ nanoplatelets EDS was used when the extent of doping was sufficient enough to be observed. To determine the bandgap (as affected by quantum confinement and halide anion) and the effect of the dopant on the electronic structure, absorbance, and photoluminescence spectroscopy were performed on the films. The hexagonal shape was then confirmed and a qualitative understanding of the size and shape distribution of the nanoplatelets was done via scanning transmission electron microscopy (STEM). EDS elemental analysis was done to understand the distribution of elements and SEM images were used to look at the physical properties of the film, both with and without laser illumination.

RESULTS

Figure 5 shows the evolution of the photoluminescence spectra over time. Spectra was

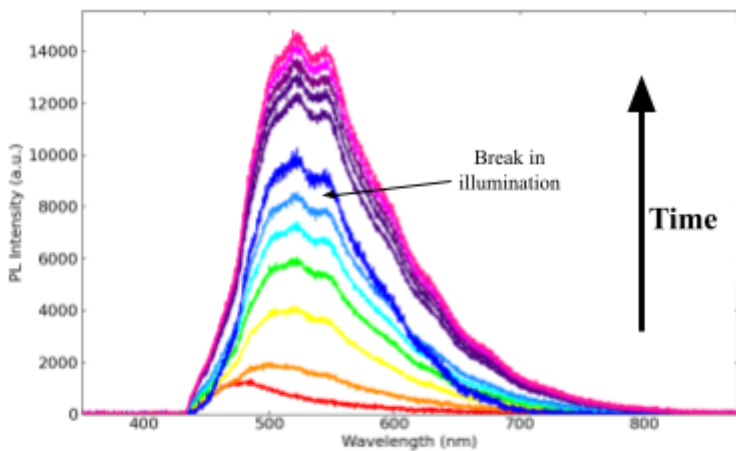


Figure 5: Photoluminescence spectra under 405 nm laser illumination with power of $11.02 \mu\text{W}$ with an integration time of 200 ms showing increasing intensity before and after a 1 second break in laser illumination.

captured every 250 ms, but for clarity, only every 50th scan is shown except for the first and seventh spectra in Figure 5 which are the 5th and 305th scan, respectively. Kinetics data was calculated by finding the maximum

point of the peak in the photoluminescence spectra between 400 and 600 nm and was set

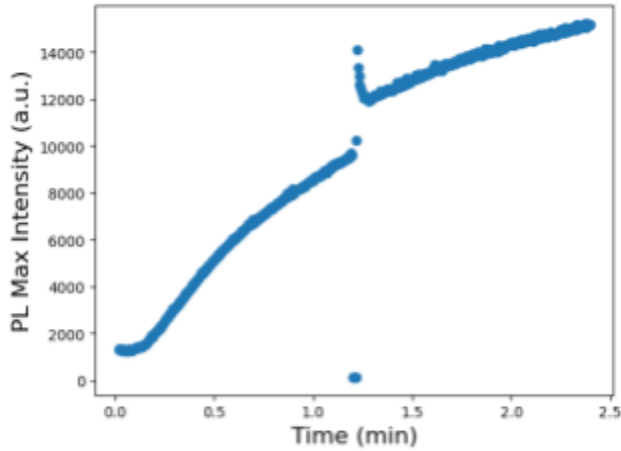


Figure 6: Kinetics analysis of maximum peak height of photoluminescence peak under 405 nm laser illumination with power of $11.02\mu\text{W}$ with an integration time of 200 ms over 2.5 minutes with data taken every 0.25 seconds.

as the maximum photoluminescence intensity for each spectra (Fig. 6). However, it should be noted that this does not take into account the change in shape that occurs as the photoluminescence intensity increases with time under continuous 405 nm laser illumination. Additionally, the break that occurs in the data at around 1.2 minutes corresponds to the laser

being blocked for a short period of time, around 1 second.

After the initial kinetics experiment, longer kinetics data was needed, so after putting the $\text{Cs}_3\text{Bi}_2\text{Br}_9:\text{Mn}$ film under 405 nm laser illumination for around 30 minutes to try to

understand the time scale that future kinetics experiments should be run on, a dark spot had formed on the film that had been under laser illumination (Fig. 7). SEM images show a section of the dark spot at different magnification levels and the bright spots that can be seen on the ridges present in the dark spot at the increased magnification level are clusters of the



Figure 7: Photograph of $\text{Cs}_3\text{Bi}_2\text{Br}_9:\text{Mn}$ film after being illuminated by a 405 nm laser for 30 minutes.

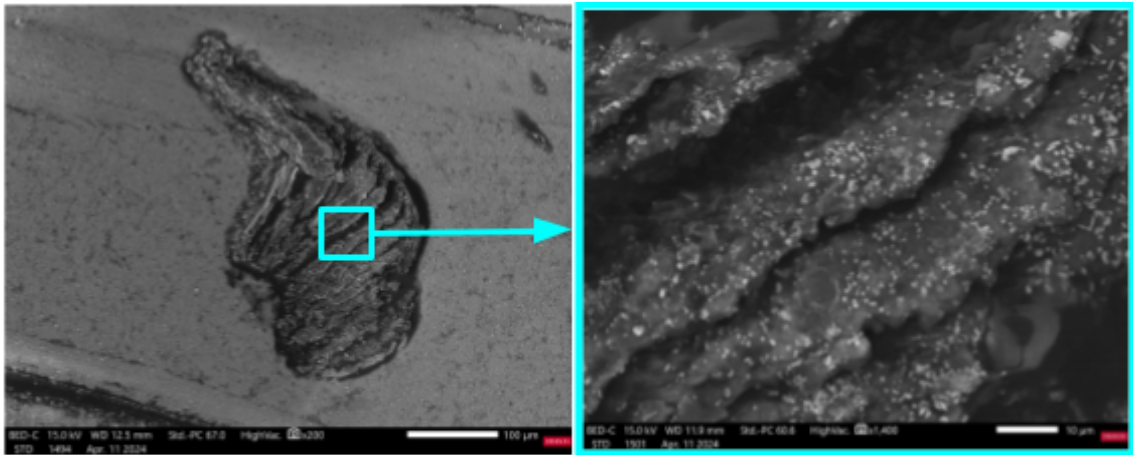


Figure 8: SEM images of dark spot of $\text{Cs}_3\text{Bi}_2\text{Br}_9:\text{Mn}$ film at different magnifications in backscatter mode with accelerating voltage of 15.0kV.

$\text{Cs}_3\text{Bi}_2\text{Br}_9:\text{Mn}$ nanoplatelets (Fig. 8). To understand if the dark spot was the absence/degradation of the sample, the dark spot was also looked at from a tilted angle using the SEM. The images show the ridges that make up the dark spot are raised and sit above the film (Fig. 9), rather than being an absence of material. Finally, an EDS elemental analysis was performed on the film to show the differences in elemental composition on the dark spot which was under 405 nm laser illumination and on the unaffected film surrounding the dark spot (Fig. 10).

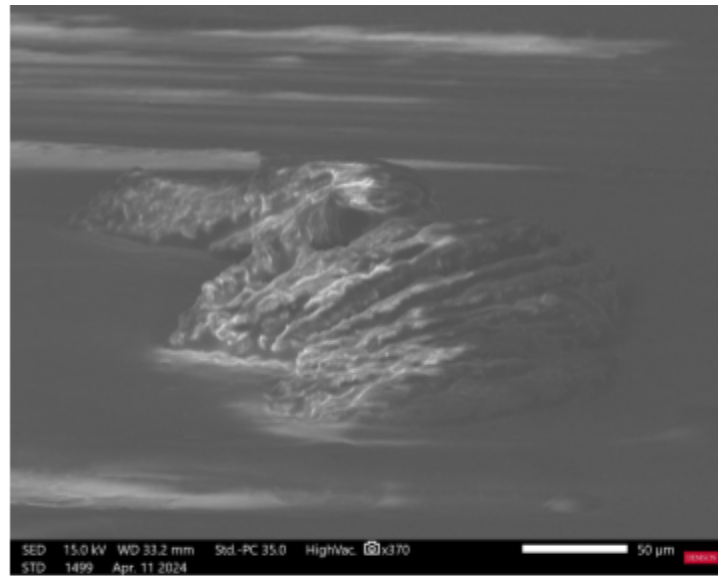


Figure 9: SEM image taken with an accelerating voltage of 15.0 kV in which the film is tilted to establish the contours of the dark spot.

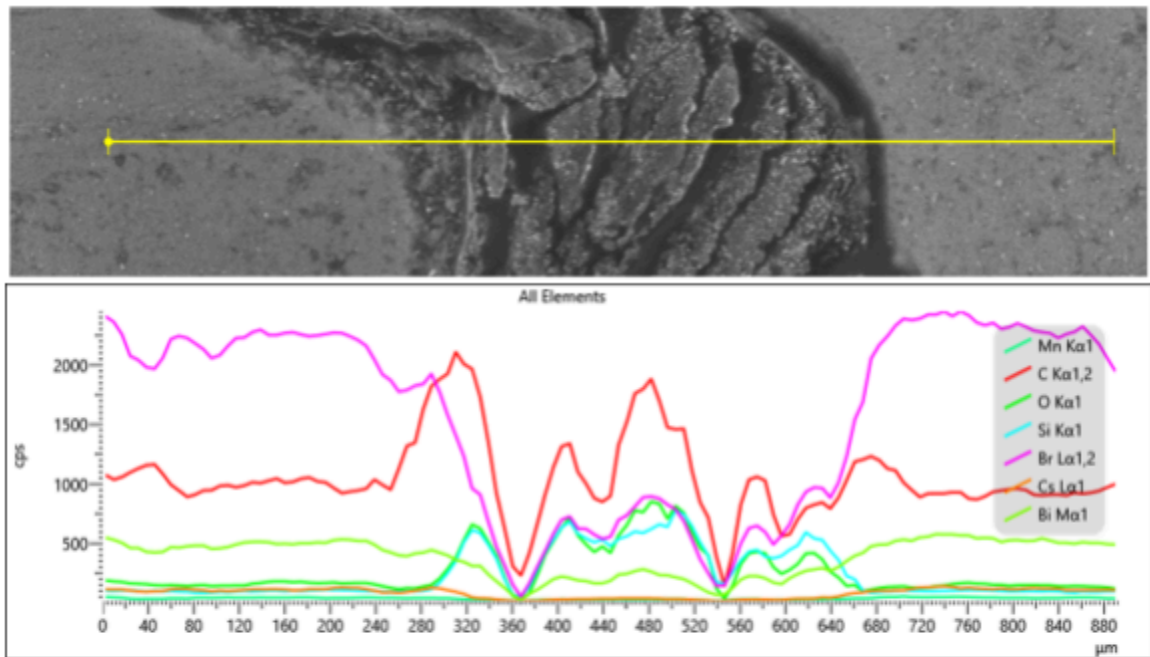


Figure 10: EDS elemental analysis across dark spot on $\text{Cs}_3\text{Bi}_2\text{Br}_9:\text{Mn}$ thin film.

DISCUSSION

The dark spot (Fig. 7) that was noticed after the film had been under laser illumination for about 30 minutes was the first indication that our previous hypotheses surrounding the brightening effect were incorrect, as it indicated a chemical change that was occurring. The EDS elemental analysis of the film (Fig. 10) showed a decrease in all elements present in the nanoplatelets and an increase in the elements present in glass when transitioning from the untouched film to the dark spot. This could be indicative of nanoplatelet degradation or an alternate reaction occurring between the nanoplatelets and the environment, leaving the glass beneath exposed. However, SEM images (Fig. 9) show clumps of the $\text{Cs}_3\text{Bi}_2\text{Br}_9:\text{Mn}$ material present in the dark spot. Heavier elements are brighter in SEM images when backscattering mode is used, and all elements present in

the nanoplatelet material are significantly heavier than the silicon and oxygen in the glass. This indicates that at least some percentage of the nanoplatelets aren't being degraded or involved in a reaction with the environment. The robustness of the nanoplatelets was unexpected, however it would be beneficial to understand if this was a characteristic present in all nanoplatelets or if this process is degrading the less robust parts of the film.

When looking at the film from an angle (Fig. 10), it can be seen that the dark spot is raised above the surrounding film. This could be explained by the glass melting, due to high laser power, and forming a matrix with the $\text{Cs}_3\text{Bi}_2\text{Br}_9:\text{Mn}$ material. The photoluminescence spectra (Fig. 5) and the corresponding kinetics analysis (Fig. 6) which was taken prior to discovering the dark spot further support this theory. The change in photoluminescence spectra peak shape as time passed could be a result of the material and/or the glass substrate heating. Also, the sharp increase in photoluminescence intensity in Figure 6 that occurs around 1.2 minutes could be indicative of a pre-melting state. During the break in laser illumination, the material would be able to cool, and when laser illumination is resumed the pre-melting emission can be seen. However, as the material begins to heat up again, there is a slight decrease in maximum photoluminescence intensity, before more of the glass begins to melt and matrix formation proceeds. However, further experimentation is necessary to confirm this hypothesis. It is also currently unknown whether the $\text{Cs}_3\text{Bi}_2\text{Br}_9:\text{Mn}$ nanoplatelets are converting light energy to heat or if waste heat produced by the laser is melting the glass substrate.

The initial photoluminescence peak (red spectra, Fig. 5) could be the $\text{Cs}_3\text{Bi}_2\text{Br}_9\text{:Mn}$ nanoplatelets. Then as illumination continues, the material and glass heat up due to the strong laser power and the photoluminescence spectra are taken over by new material.

The high laser power was necessary to see the initial weak emission of the material, however further experimentation could be done with variation in laser power.

Another important aspect in the EDS elemental analysis (Fig. 10) to note is the lack of Mn present in any part of the film which calls into question the effectiveness of the Mn-doping. Although, the undoped material doesn't exhibit the same brightening effect under the same experimental condition (Fig. 2). This could be explained by the relative differences in the amount of Mn present in the sample compared to all other elements present in the material and in the glass. However further experimentation is needed to understand if this is an effect which is unique to a film of the Mn-doped nanoplatelets on glass.

FUTURE WORK

To understand if this effect is unique to the $\text{Cs}_3\text{Bi}_2\text{Br}_9\text{:Mn}$ nanoplatelets on glass, future experiments are needed. Extended 405 nm laser illumination of the Mn-doped $\text{Cs}_3\text{Bi}_2\text{Br}_9$ nanoplatelet film on a sapphire substrate could be an initial experiment. Sapphire has a higher melting point than glass and this would explain if glass and/or the substrate melting is necessary for the brightening effect to occur. Similarly, looking at dark spot formation as a function of 405 nm laser power could explain if the laser is causing the glass to melt. The formation of the dark spot would only start once a certain power threshold was reached, regardless of exposure time. Also, taking SEM images that show

the contour of the film as well as EDS elemental mapping and analysis after different time periods under laser illumination would allow for a better understanding of the physical changes in the film and substrate, as well as changes in elemental makeup of the top layer of the film. Finally, using $\text{Cs}_3\text{Bi}_2\text{Br}_9$ nanoplatelet samples with varying Mn-dopant levels, as well as an undoped sample would allow us to understand if the addition of manganese is necessary for the brightening effect to be observed.

REFERENCES

- (1) Shamsi, J.; Urban, A. S.; Imran, M.; De Trizio, L.; Manna, L. Metal Halide Perovskite Nanocrystals: Synthesis, Post-Synthesis Modifications, and Their Optical Properties. *Chem. Rev.* **2019**, *119* (5), 3296–3348. <https://doi.org/10.1021/acs.chemrev.8b00644>.
- (2) Schmidt, L. C.; Pertegás, A.; González-Carrero, S.; Malinkiewicz, O.; Agouram, S.; Mínguez Espallargas, G.; Bolink, H. J.; Galian, R. E.; Pérez-Prieto, J. Nontemplate Synthesis of CH₃NH₃PbBr₃ Perovskite Nanoparticles. *J. Am. Chem. Soc.* **2014**, *136* (3), 850–853. <https://doi.org/10.1021/ja4109209>.
- (3) Protesescu, L.; Yakunin, S.; Bodnarchuk, M. I.; Krieg, F.; Caputo, R.; Hendon, C. H.; Yang, R. X.; Walsh, A.; Kovalenko, M. V. Nanocrystals of Cesium Lead Halide Perovskites (CsPbX₃, X = Cl, Br, and I): Novel Optoelectronic Materials Showing Bright Emission with Wide Color Gamut. *Nano Lett.* **2015**, *15* (6), 3692–3696. <https://doi.org/10.1021/nl5048779>.
- (4) Fan, Q.; Biesold-McGee, G. V.; Ma, J.; Xu, Q.; Pan, S.; Peng, J.; Lin, Z. Lead-Free Halide Perovskite Nanocrystals: Crystal Structures, Synthesis, Stabilities, and Optical Properties. *Angewandte Chemie International Edition* **2020**, *59* (3), 1030–1046. <https://doi.org/10.1002/anie.201904862>.
- (5) Ghosh, S.; Pradhan, B. Lead-Free Metal Halide Perovskite Nanocrystals: Challenges, Applications, and Future Aspects. *ChemNanoMat* **2019**, *5* (3), 300–312. <https://doi.org/10.1002/cnma.201800645>.
- (6) Xu, L.; Yuan, S.; Zeng, H.; Song, J. A Comprehensive Review of Doping in Perovskite Nanocrystals/Quantum Dots: Evolution of Structure, Electronics, Optics, and Light-Emitting Diodes. *Materials Today Nano* **2019**, *6*, 100036. <https://doi.org/10.1016/j.mtnano.2019.100036>.
- (7) Liu, W.; Lin, Q.; Li, H.; Wu, K.; Robel, I.; Pietryga, J. M.; Klimov, V. I. Mn²⁺-Doped Lead Halide Perovskite Nanocrystals with Dual-Color Emission Controlled by Halide Content. *J. Am. Chem. Soc.* **2016**, *138* (45), 14954–14961. <https://doi.org/10.1021/jacs.6b08085>.
- (8) Creutz, S. E.; Liu, H.; Kaiser, M. E.; Li, X.; Gamelin, D. R. Structural Diversity in Cesium Bismuth Halide Nanocrystals. *Chem. Mater.* **2019**, *31* (13), 4685–4697. <https://doi.org/10.1021/acs.chemmater.9b00640>.